JOURNAL OF MATERIALS SCIENCE: MATERIALS IN ELECTRONICS **14** (2003) 407–411

Low-temperature PECVD deposition of highly conductive microcrystalline silicon thin films

A. M. NARDES, A. M. DE ANDRADE, F. J. FONSECA, E. A. T. DIRANI
LME. Dept. Eng. Sist. Eletr., Escola Politécnica da USP, São Paulo, SP, Brazil
E-mail: alemn@lme.usp.br

E. A. T. DIRANI
Dept. de Eng. Eletr., Pontificia Universidade Católica de São Paulo, SP, Brazil

R. MUCCILLO, E. N. S. MUCCILLO
CMDMC, CCTM, Instituto de Pesquisas Energéticas e Nucleares, São Paulo, SP, Brazil

In this paper, we present the characterization results of doped n-type microcrystalline hydrogenated-silicon (μc-Si : H) films deposited in a plasma-enhanced chemical vapor deposition in the temperature range between 70 and 250 °C. The interest in these films arises from the fact that they combine the high optical absorption of amorphous silicon with the electronic behavior of the crystalline silicon, making them interesting for the production of large electronic devices such as solar cells, image sensors, and flat panels. It is shown that n-type μc-Si : H films with high electrical conductivity can be obtained even at low temperature deposition, around 120 °C ($\sigma = 2.9\ \mathrm{S\,cm^{-1}}$). The structural properties of the films have been studied by Raman and infrared spectroscopy that allowed for the determination of the crystalline fraction. Electrical measurements were performed by a.c. impedance spectroscopy, Hall effect, and dark conductivity. Characteristics suitable for application in electronic devices were obtained with the developed deposition parameters set-up; the best dark conductivity values were around $1\ \mathrm{S\,cm^{-1}}$ for deposition temperatures within the 120–140 °C range. Some conclusions regarding the correlation between electrical and structural properties are presented for the considered temperature range.
© *2003 Kluwer Academic Publishers*

1. Introduction

In order to fabricate reliable, thin film transistors or solar cells at low cost, with acceptable conversion efficiency, several groups around the world directed their efforts to the research of microcrystalline hydrogenated-silicon films (μc-Si : H) developing a new material with good optical and electrical properties [1]. Since then, the applications of this promising material in solar cells or thin film transistors have been achieved with good results. Low-temperature deposition methods are needed for producing large-area electronics on alternative and low-cost substrates such as polymers.

It is well known that μc-Si : H films have an amorphous silicon matrix in which silicon crystalline grains are embedded [2]. The electrical conductivity of this inhomogeneous material is a result of the contribution of the different regions of the material. To extract a correlation between morphological and electrical properties, we combine structural measurement techniques (Raman and infrared spectroscopy) with electrical measurement techniques (Hall effect, d.c. conductivities and impedance spectroscopy). Impedance spectroscopy gives information on the material structure (the contribution of each phase to the overall conductivity) from electrical measurements using alternating current in a wide frequency range, overcoming the limitations imposed by the d.c. measurements that gives only the total electrical conductivity. More recently, this technique has been utilized in the analysis of amorphous and microcrystalline silicon [3].

The impedance spectroscopy technique consists usually in the measurement of the impedance (Z) as a function of the frequency f of the input signal over a frequency range. The data [4] are obtained as a Cole–Cole plot (the imaginary component of the impedance, Z'' as a function of the real part of the impedance, Z'). It is possible to separate the contributions of the different phases of the material in the frequency domain according to their characteristic relaxation times. The data extracted from the measurements are: the electrical resistance of each component of the system, the characteristic relaxation frequency ω_0, the relaxation time τ (equal to the RC constant of the electrical circuit) and the decentralization angle ϕ, which can be related to the microscopic homogeneity of the μc-Si : H films [3].

Fig. 1 shows an impedance diagram and its equivalent electrical circuit for a resistance r connected in series with two RC sets in parallel.

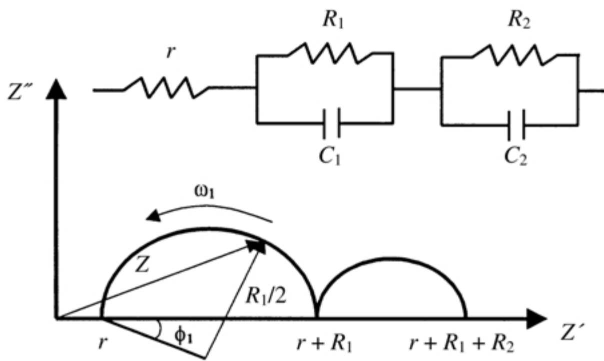

Figure 1 Impedance diagram of an equivalent electrical circuit for a resistance "r" connected in series with two "RC" sets in parallel.

In this paper, the correlation between the substrate temperature, structural properties, and electric conductivity has been investigated in μc-Si : H.

2. Experimental

For the present study, two sets of samples were deposited in a single-chamber PECVD reactor (13.56 MHz) with an r.f. triode-coupling configuration. In the first set, n-type μc-Si : H layers films were deposited onto Corning Glass 7059 and p-type single-crystal silicon (7–13 Ω cm) substrates. The deposition conditions were: H_2 flow rate = 200 sccm, SiH_4 dilution = 0.8%, PH_3 dilution = 0.5%, deposition pressure = 13 pa, r.f. power density = 125 mW cm^{-2}, deposition time = 60 min. The substrate temperature was varied between 100 and 250 °C. In the second set of depositions, the n-type Si-μc : H films were deposited onto glass substrates under the following deposition conditions: H_2 flow rate = 250 sccm, SiH_4 and PH_3 dilution = 1.0%, deposition pressure 13 Pa, r.f. power density 62.5 mW cm^{-2}, deposition time = 120 mins and substrate temperature range between 70 and 150 °C.

The crystalline fraction and the average grain sizes were obtained from Raman scattering measurements using a microRaman spectrometer (Renishaw Imaging Microscope – model U3000) using the 632.8-nm line of a He–Ne laser. The laser line was focused on the sample (1 μm area) through a microscope (Olympus BTH-2) attached to a charge couple device (CCD) camera. The power output of the laser was 40 mW to avoid thermally inducing crystallization. The crystalline volume fraction (X_c) was estimated by the deconvolution of the spectra into amorphous, transition phase, and crystalline components.

The electrical properties: dark conductivity (σ_d), impedance as a function of frequency from 6 to 13 MHz (HP 4192A impedance analyzer) and Hall effect, have been measured at room temperature. Evaporated aluminum contacts were deposited onto glass substrate to form the electrodes. For dark conductivity, σ_d, and impedance spectroscopy measurements, two rectangular and parallel coplanar electrodes were used. The van der Pauw contacts configuration [5] was employed to determine carrier concentration (N_H) and electrical conductivity (σ_H) using a Biorad HL5500PC Hall measurement equipment.

3. Results and discussion

The results of the characterization of two sets of deposited samples are presented. The samples in the two sets differ in their deposition parameters. In the second set of samples the deposition parameters were tuned aiming to obtain higher electrical conductivity on films deposited at lower temperature.

3.1. First set of samples

The electrical and structural characteristics of samples deposited between 100 and 250 °C are presented and discussed.

3.1.1. Structural analysis

Fig. 2 shows the Raman spectra of the first set of samples. The existence of an amorphous phase in the matrix is responsible for a distribution of lengths and angles in the silicon-to-silicon bonds [6]. As a consequence, there is a broadening in the Raman spectra as well as a shift to lower energies. We observed that, with decreasing deposition temperature, the crystalline component (520 cm^{-1}) broadens and its maximum shifts to lower frequencies.

The crystalline fraction (X_c) obtained from the deconvolution of the Raman spectra for wave numbers between 480 and 520 cm^{-1} attributed to the vibrational TO modes [7] of the network phonons on the amorphous and crystalline silicon, respectively, has a quasi-linear dependence with the temperature. The crystalline fraction (X_c) was calculated through the empiric expression [8] $X_c = (I_c + I_m)/(I_c + I_m + I_a)$, where I_c corresponds to the integrated intensity of the 520 cm^{-1} peak, ascribed to the crystalline contribution; I_m is the integrated intensity in the Gaussian related to the intermediate peak 510 cm^{-1}, and I_a is the integrated intensity of the 480 cm^{-1} peak, ascribed to the amorphous sections of the material. Fig. 3 shows the deconvoluted spectrum that allows for the calculations of the crystalline phases. In the calculation of X_c the intermediate 510 cm^{-1} peak was assumed to be related to grain boundaries, where an increase in the bond lengths of the crystalline regions shifts the Raman dispersion spectra to lower energies. With this procedure, more reliable results are obtained since all the contributions from the material structure are taken into

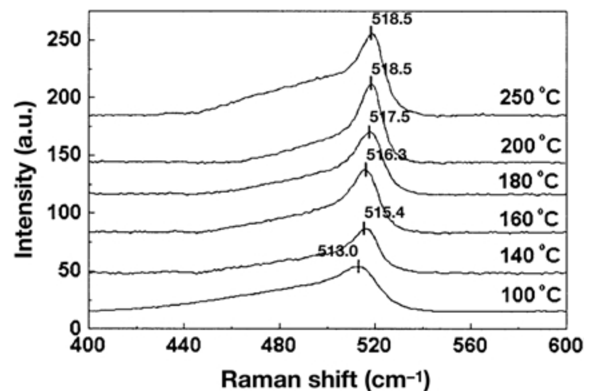

Figure 2 Raman spectra of films deposited in the temperature range within 100 and 250 °C.

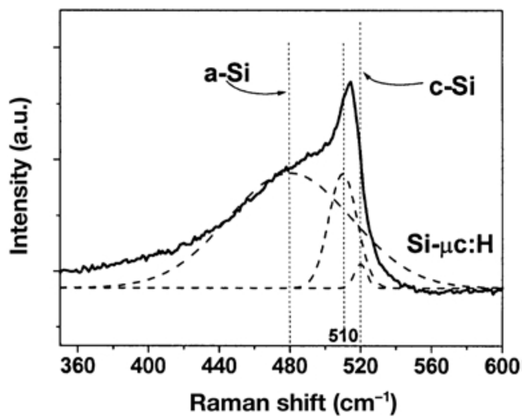

Figure 3 Raman dispersion of microcrystalline hydrogenated-silicon samples showing the deconvolution of spectrum for crystalline ($520\,cm^{-1}$), intermediate ($510\,cm^{-1}$), and amorphous ($480\,cm^{-1}$) phases.

account in the matrix phonon scattering for the Raman spectra deconvolution [6, 9, 10].

Crystalline fractions up to 30% were obtained at temperatures below 100 °C. As the deposition temperature increased, the maximum crystalline fraction was approximately 80% in our samples.

This crystalline volume fraction value confirms the supposition [11] about the structural relaxation to a more stable configuration (crystalline) with an increase in the mobility of the species adsorbed in the growing surface. It is worth noting that these crystallinity fractions (66% at $T_s = 100\,°C$ for undoped samples) are obtained at temperatures lower than those usually used in the CVD microcrystalline silicon film deposition process. This is an indication that there are factor(s) affecting the crystallization mechanisms other than the substrate deposition temperature [12].

The way the hydrogen is incorporated in the network can be indicative of the film structure. The infrared spectra shown in Fig. 4 shows that with an increase of the deposition temperature there is a decrease in the stretching absorption modes at 2000 and $2100\,cm^{-1}$ (Si–H and $Si–H_2$, respectively) and also at $\sim 630\,cm^{-1}$, characteristic of the bending, rocking, and wagging modes, ascribed to the Si–H bonds [13].

A reduction of the absorption at $890\,cm^{-1}$ is also observed. The interpretation of the $Si–H_x$ ($x = 1$, 2 or 3 modes) associated with this spectral region is as follows: the absorption at $890\,cm^{-1}$ (''scissors''–''wagging'')

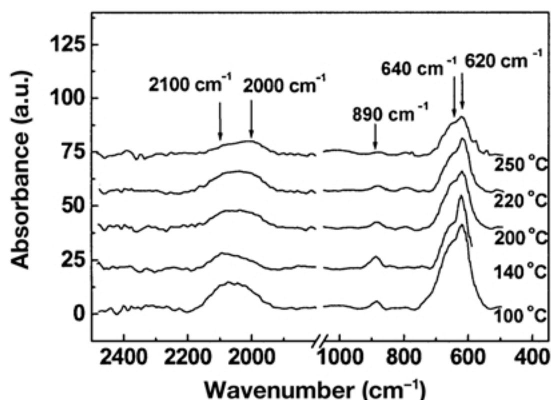

Figure 4 Infrared spectra of films deposited in the temperature range 100 to 250 °C.

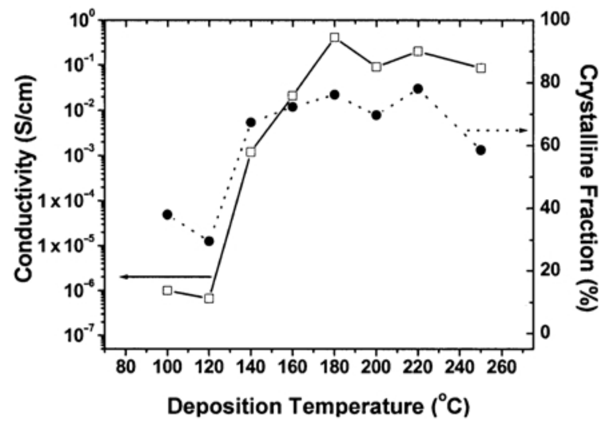

Figure 5 Conductivity and crystalline fraction as a function of the substrate temperature for representative hydrogenated-silicon films. ● Crystalline fraction, □ Conductivity.

and at 2090–$2100\,cm^{-1}$ (''stretching'') is ascribed to the presence of $[Si–H_2]_n$ type of bonds, whilst the absorption at $880\,cm^{-1}$ and $907\,cm^{-1}$ is ascribed to the ''bending'' modes of hydrogen bonded as $Si–H_2$ and $Si–H_3$.

A possible interpretation for the observed result is that at higher temperatures the precursors are more energetic and, as a consequence, due to their greater mobility, a rearrangement to a more stable configuration in the growing surface occurs [14].

3.1.2. D.C. conductivity

Fig. 5 shows that the electrical conductivity exhibits an increase of five orders of magnitude when the substrate deposition temperature is increased from 120 to 180 °C, with the crystalline fraction showing a similar behavior.

The measured d.c. conductivity values for samples deposited at temperatures below 140 °C are smaller than the typical conductivities of n-type doped amorphous silicon [15] films ($\sim 10^{-2}\,S\,cm^{-1}$). Some hypotheses to explain this fact are presented in the literature: (a) the phosphorus atoms are not activated due to the low substrate deposition temperatures utilized in the preparation of the samples with a consequent reduction in the number of carriers [16]; (b) the phosphorus atoms in interstitial structure [17] sites contribute to increase the structural defect density, thus reducing the electronic mobility and are segregated to the amorphous matrix region around the crystallites impairing the electric conduction process, and (c) the properties of the amorphous matrix depend both on the hydrogen content and on the hydrogen–silicon bond properties. Considering just the samples deposited at temperatures above 140 °C, we observe that the density of carriers, as evaluated by Hall effect measurements, is proportional to the crystalline volume fraction of the film (Fig. 6).

3.1.3. Impedance measurements

Complex impedance diagrams of Z'' (Ω) as a function of Z' (Ω), i.e., Cole–Cole plot [18], are presented in Fig. 7 for the Al/μc-Si:H/A1 structure deposited in the temperature range of 180–250 °C. The measurements were carried out at room temperature. The simplest equivalent circuit describing the impedance of a two-

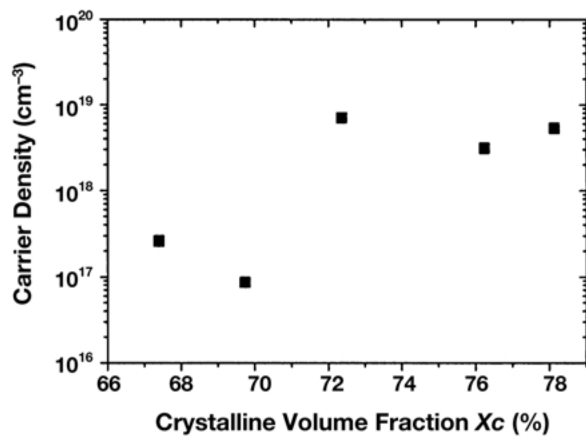

Figure 6 Carrier density as function of the crystalline volume fraction X_c (%).

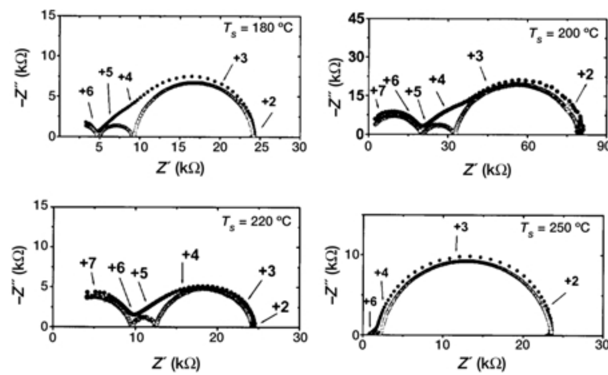

Figure 7 Room-temperature impedance spectra of μc-Si : H deposited at different temperatures. The arrows indicate the logarithm of the frequency. ● Experimental, ○ Deconvolution.

phase material (e.g., amorphous/microcrystalline silicon) is composed of two circuits in series, each one a capacitor in parallel with a resistor. The impedance of this circuit as a function of frequency gives two semicircles in the complex plane. The decentralization angle, ϕ, may be an indication of the degree of homogeneity of the material [4]. The larger the angle, the more non-uniform is the distribution of crystallite sizes in the amorphous matrix. The center of a semicircle is frequently shifted below the real axis due to the effect of the inhomogeneity of the specimen.

We can observe that only for the sample deposited at 250 °C there are two semicircles in the complex diagram.

Fig. 8(a) shows the relationship between ϕ and the hydrogen content. This behavior is consistent with the idea that ϕ is a parameter that indicates the microscopic homogeneity of the sample. Higher hydrogen content values leads to a higher structural disorder of μc-Si : H

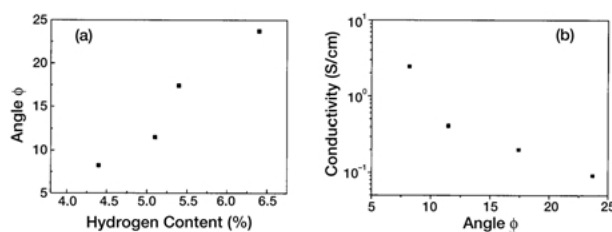

Figure 8 (a) Decentralization angle as a function of hydrogen content calculated from IR spectra; (b) dependence of the d.c. conductivity on the decentralization angle ϕ.

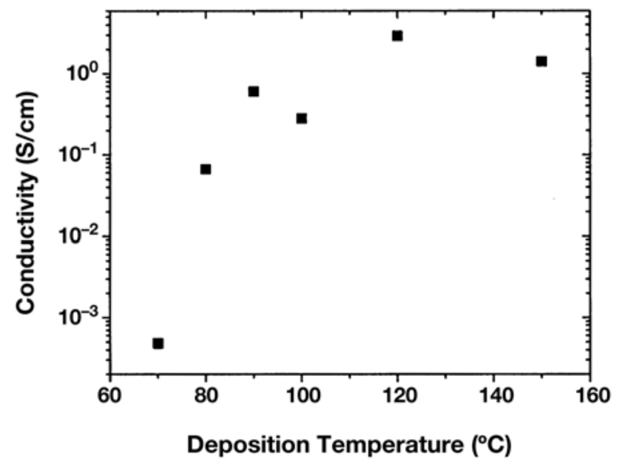

Figure 9 Dark conductivity of μc-Si : H as a function of the deposition temperature.

films. The conductivity is also related to the ϕ angle as Fig. 8(b) shows.

The conductivity σ is obtained from Z_0 by means of the relation $\sigma = (1/Z_0)(l/S)$, where l/*S* represents the sample geometric factor (l = electrodes distance and S = electrode width versus film thickness).

3.2. Second set of samples

In the second set of samples we fine tuned the deposition parameters to achieve higher conductivity. The results are shown in Fig. 9.

Comparing these results with the results obtained in the first set of deposited samples, an increase in the conductivity values for the samples deposited at temperatures below 150 °C can be seen.

4. Conclusions

It has been shown that the substrate temperature deposition is not a *sine-qua-non* condition to produce microcrystalline hydrogenated-silicon films. With the proper choice of deposition parameters, deposition at low temperature of microcrystalline silicon films exhibiting high conductivity is possible in a conventional PECVD reactor, like the one utilized.

We observed that a sudden increase in the dark conductivity occurs at around 140 °C. We did not observe, however, a corresponding increase in the average grain size nor in the crystalline volume fraction, which shows an almost linear increase with the deposition temperature. The influence of the temperature on the electrical conductivity of the μc-Si : H films may be related to the phosphorus activation, which increases with increasing deposition temperatures.

The increase in the electrical conductivity depends on an increased incorporation of the phosphorus dopant in a P_4 configuration (coordination number 4). If there is insufficient energy in the system to permit the phosphorus atoms to bond in this configuration, they will be interstitially located, increasing the defect density, or they may segregate to the grain boundaries in a P_3 configuration [17]. In both cases, the result is a

decrease of the crystallinity and the conductivity of the samples.

For the lower substrate deposition temperatures, the precursor adatom species ($Si–H_3$, $Si–H_2$, Si–H, $P–H_2$, P–H, H) mobility is smaller than at higher deposition temperatures [19]. Hydrogen bonded to a crystalline grain may act as a barrier, inhibiting grain growth [2]. Also, due to the chemical reactivity of the hydrogen plasma with silicon, the formation of polymer-like chains $[Si–H_2]_n$ may occur [20]. This situation leads to a reduction in the electrical conductivity and, to a smaller degree, in the crystalline volume fraction.

Although it is still difficult to interpret the phenomena leading to the appearance of three semicircles in the impedance spectra, the impedance spectroscopy can be used to separate the different contributions of the phases to the electrical resistivity of the material. Considering that the material is composed of small crystals embedded in an amorphous tissue, there should be contributions of the crystalline material, of the amorphous phase, of the crystalline to the amorphous interface, as well as of their interface with the metallic electrodes (blocking or not).

Acknowledgments

The authors thank FAPESP for the financial support. The authors are indebted to Dr Paulo S. Santos and Dr Lucia K. Noda from the Instituto de Química da Universidade de São Paulo for the Raman analysis.

References

1. O. VERTTERL, F. FINGER, R. CARIUS, P. HAPKE, L. HOUBEN, O. KLUTH, A. LAMBERTZ, A. MÜCH, B. RECH and H. WAGNER, *Sol. Energy Mater. Sol. Cells* **62** (2000) 97.
2. Y. MISHIMA, S. MIYAZAKI, M. HIROSE and Y. OSAKA, *Philos. Mag. B* **46** (1982) 1.
3. P. Y. TIMBRELL, B. RANCHOUX and H. HAMDI, *J. Non-Cryst, Solids* **64** (1984) 21.
4. J. ROSS MACDONALD, in ''Impedance Spectroscopy: Emphasing Solid Materials and Systems'' (John Wiley & Sons, 1987).
5. R. MARTINS, A. A. MAÇARICO, I. FERREIRA, R. NUNES, A. BICHO and E. FORTUNATO, *Thin Solid Films* **303** (1997) 47.
6. S. VEPREK, F. A. SAROT and Z. IQBAL, *Phys. Rev. B* **36** (1987) 3344.
7. M. LUYSBERG, P. HAPKE, R. CARIUS and F. FINGER, *Philos. Mag. A* **75** (1997) 31.
8. T. KANEKO, M. WAKAGI, K. ONISAWA and T. MINENMURA, *Appl. Phys. Lett.* **64** (1994) 1865.
9. M. WAKAGI, T. KANEKO, K. OGATA and A. NAKANO, *Proc. Mater. Res. Symp.* **283** (1993) 555.
10. E. A. T. DIRANI, A. M. ANDRADE, L. K. NODA, F. J. FONSECA and P. S. SANTOS, *J. Non-Cryst. Solids* **273** (2000) 307.
11. K. KOMOTO, Y. URANO, J. L. GUIZOT, G. GANGLY and A. MATSUDA, *Jpn. J. Appl. Phys.* **30** (1991) L790.
12. P. ROCA, I. CABARROCAS, N. LAYADI, B. DREVILLON and I. SOLOMON, *J. Non-Cryst. Solids* **198–200** (1996) 871.
13. P. J. ZANZUCCHI, in ''Semiconductors and Semimetals'' **21**, part B (Academic Press, Inc., Princeton, New Jersey, 1984) p. 121.
14. P. APUIM, V. CHU and J. P. CONDE, *J. Appl. Phys.* **86** (1999) 3812.
15. P. G. LECOMBER, D. I. JONES and W. E. SPEAR, *Philos. Mag.* **35** (1977) 1173.
16. F. J. FONSECA, R. GALLONI and A. N. LARSEN, *Philos. Mag. B* **63** (1993) 107.
17. D. ADLER, in ''Semiconductors and Semimetals'' **21**, part A (Academic Press, Inc., Princeton, New Jersey, 1984) p. 306.
18. K. S. COLE and R. H. COLE, *J. Chem. Phys.* **9** (1941) 341.
19. C. C. TSAI, G. B. ANDERSON and R. THOMPSON, in *Proc. Mater. Res. Soc. Symp.* **192** (1990) 475.
20. F. J. KAMPAS, *J. Appl. Phys.* **20** (1982) 6408.

Received 10 June 2002